Technical Document 3268
March 2013

Absorption-induced Optical Tuning of Silicon Photonic Structures Clad with Nematic Liquid Crystals

J. N. Ptasinski

Approved for public release.

SSC Pacific
San Diego, CA 92152-5001

Technical Document 3268
March 2013

Absorption-induced Optical Tuning of Silicon Photonic Structures Clad with Nematic Liquid Crystals

J. N. Ptasinski

Approved for public release.

SSC Pacific
San Diego, CA 92152-5001

SSC Pacific
San Diego, California 92152-5001

J.J. Beel, CAPT, USN
Commanding Officer

C. A. Keeney
Executive Director

ADMINISTRATIVE INFORMATION

This report was prepared for the Office of Naval Research (ONR) Naval Innovative Science and Engineering (NISE) Program by the Advanced Photonics Technology Branch (Code 55360) and the Wireless Communications Branch (Code 55310), SPAWAR Systems Center Pacific, San Diego, CA.

Released by
A. D. Ramirez, Head
Advanced Photonics Technology
Branch

Under authority of
C. Hendrickson, Head
Enterprise Communications
& Networks Division

This is a work of the United States Government and therefore is not copyrighted. This work may be copied and disseminated without restriction.

COMSOL Multiphysics® [i] is a registered trademark of COMSOL.
Plasmalab 100® is a registered trademark of Oxford Instruments.

SB

CONTENTS

INTRODUCTION **1**

DESIGN AND ANALYTICAL MODEL **5**

DEVICE FABRICATION AND CHARACTERIZATION **7**

SUMMARY **11**

REFERENCES **13**

Figures

1. (A) Ring resonator. Windows for liquid crystal cladding are etched within the silicon dioxide over-cladding. (B) Simulation result showing critical coupling that translates to a resonance peak. 4
2. (A,B) Simulation result for the TE mode, (B) the simulated ring resonator structure and its TM mode response. 6
3. Fabrication process steps for devices with a photo-voltage liquid crystal cladding. The dimensions are not to scale 7
4. Fabricated ring resonator structures. (A) Gap between the ring and bus wave-guide; (B) Ring resonator; (C) Fabricated leads for electrodes; (D, E) Etched silicon dioxide cladding to allow room for liquid crystals; (F) 45-degree view of the waveguide sidewalls (250-nm tall); (G) Tip of the inverse taper; (H) 85-degree view of the ring sidewalls. 8
5. Experimental setup 10
6. Experimental results of 5CB liquid crystal doped with methyl red dye 11

INTRODUCTION

Photo-manipulation of nematic liquid crystal orientation has attracted considerable attention due to its applications in the non-contact, high-resolution alignment of liquid crystal display (LCD) cells. Nematic liquid crystals are known for their unusually large nonlinear optical properties, where the optically induced liquid crystal axis reorientation is possible using low-threshold laser powers, thereby lending to their increasing use in many opto-electronic image sensing, display, and processing devices [1]. This technical document demonstrates photo-tuning of silicon structures clad in a nematic liquid crystal in the presence of low-power photo irradiation.

Silicon photonics is an evolving field allowing for optical devices to be made cost effectively using standard semiconductor fabrication techniques, which in turn enables integration with microelectronic chips. The rise in Internet and data transmission, the need for higher speed, broader bands, and lower cost are driving silicon photonic technologies, which offer transfer rates of 25 gigabits per second between computer chips in servers, large data centers, and supercomputers, in addition to proffering dramatic costs savings in materials, components, and energy consumption.

As new silicon photonic devices emerge, liquid crystals are poised to find applications in active modulation of silicon waveguides and switches. Tunable optical circuit components are one of the essential technologies in the development of photonic analogues for classical electronic devices, since using one tunable device replaces many single wavelength devices and therefore minimizes the space occupied on-chip [2, 3]. As silicon photonics and all-optical platforms advance, optically tunable devices are poised to play an increasingly central role.

Active tuning of modulators and ring resonator silicon photonic devices has been demonstrated using thermal, electrical, and optical means. Specifically, optical tuning of silicon ring resonators was achieved by injection of free carriers through two-photon absorption using 10-ps pump pulses [4]. Optical properties of silicon can also be modified by changing the refractive index of a material that is infiltrated inside a host silicon matrix [5].

This work presents a complementary metal-oxide-semiconductor (CMOS)-compatible, active optical-tuning scheme for silicon devices using silicon strip waveguides combined with nematic liquid crystal (NLC) claddings. A nematic liquid crystal possesses properties between those of a conventional liquid and those of a solid. Nematics in their liquid phase consist of elongated molecules which, on average, are oriented parallel to one another in their ground state. Nematic liquid crystals are strongly anisotropic substances characterized by a high degree of long-range orientational order but no translational order.

Uniformly aligned, positive birefringence nematics are optically uniaxial with $n_e > n_o$, where $\Delta n = n_e - n_o$ [1]. To change the liquid crystal (LC) orientation an electric or magnetic field is applied, where to minimize the electrostatic energy, liquid crystals align their long axis parallel to the applied field. The initial ordering of liquid crystal molecules without an external field is determined by the anisotropy of the boundary. In a typical liquid crystal cell, such as an LCD display, the surface of the electrodes is coated with an alignment layer that is then rubbed with a velvet cloth to generate grooves within the alignment layer. Liquid crystal molecules then align with their long axis parallel to the rubbing direction and depending on the boundary conditions and the molecular interaction between the liquid crystal molecules, a

long-range ordering of the molecular orientation may exist throughout the liquid crystal cell [6].

Mesogenic molecules or organic molecules forming liquid crystalline phases do not possess excess electric charge, but the charge distribution within different parts of the molecule may vary. When one end of the liquid crystal molecule is positively charged and the other end is negatively charged, the molecule becomes a dipole [7]. All atoms and molecules can be polarized by an electric field, consequently changing their shape and orientation in mesophases as well as in isotropic liquids or crystalline solids [8]. When an electric field is applied, it deforms the charge distribution of the liquid crystal molecule, and as a result an additional dipole appears. The orientation of director, **n**, starts changing as the applied electric field rises over a critical value known as the Freedericksz transition, first observed by Freedericksz and Repiewa in 1927. Positive anisotropy liquid crystals will align their long axis parallel to the applied field, while negative dielectric anisotropy liquid crystals will turn in the direction normal to the applied field. By virtue of collective molecular behavior, this response is more pronounced in a mesophase as compared to the isotropic phase.

In the presence of a uniform local electric field **E**, the torque **Γ** induced on a neutral molecule with a charge distribution $e_\alpha(\mathbf{r}_\alpha)$ can be described by

$$\mathbf{\Gamma}_{\mathrm{Elec}} = \mathbf{p} \times \mathbf{E}, \tag{1}$$

where **p** is the dipolar moment and the potential energy of the molecule is [8]:

$$U(\mathbf{E}) = -\mathbf{p}.\mathbf{E}. \tag{2}$$

The propensity of the director to take on a particular spatial distribution can be described by the Oseen–Frank elastic continuum theory where elastic forces arising from the molecular structure resist any distortion to the director field from its equilibrium state. To distort the director field, an interaction with external fields or confining surfaces is required.

In the case of an isolated dipole, the local electric field can differ significantly from the overall applied field due to the contribution of a large number density N of neighboring dipoles. The torque exerted on the director as a result of the applied macroscopic field is then

$$\mathbf{\Gamma}_{\mathrm{Elec}} = N \langle \mathbf{p} \times \mathbf{E} \rangle = \mathbf{P} \times \mathbf{E}, \tag{3}$$

where **P** is the polarization proportional to the macroscopic field **E**.

The polarization of the anisotropic medium can be further defined as

$$P_i = \varepsilon_o \kappa_{ij} E_j, \tag{4}$$

where κ_{ij} is the dielectric susceptibility tensor described by two parts $\kappa_{ij} = \kappa_{ij}^{\ \mathrm{iso}} + \kappa_{ij}^{\ \mathrm{aniso}}$ isotropic and anisotropic. We then have

$$\mathbf{P} = \mathbf{P}^{\ \mathrm{iso}} + \mathbf{P}^{\ \mathrm{aniso}}. \tag{5}$$

Since $\mathbf{P}^{iso}$ is parallel to **E**, only the anisotropic part of the susceptibility can give a torque. When the dielectric anisotropy of $\varepsilon_{\parallel}$ and $\varepsilon_{\perp}$, measured with **E** parallel and perpendicular to the director **n**, is $\varepsilon_{\parallel} - \varepsilon_{\perp} > 0$, the torque tends to align the director with the field.

If $\varepsilon_{\parallel} - \varepsilon_{\perp} < 0$, the torque will align the director normal to the field [8].

Under the presence of a sinusoidal alternating current (AC) electric field, molecular reorienting can take place if the frequency is low enough. If the frequency is too high, only the intramolecular motions are able to follow the field, due to the frequency dependence of reorientation time.

Orientation in the presence of an optical field is analogous to low-frequency AC electric field reorientation. The mechanism of this light-induced reorientation phenomena is associated with interaction between the electric field of the light beam and the incited electrical polarization of nematic molecules [9]. The electromagnetic field exerts a torque on the liquid crystal molecules due to their anisotropic molecular polarizibility; this torque is balanced by the elastic and viscous torque associated with the spatial nonuniformity and rotation of the nematic director [10]. Among optical materials, liquid crystals are highly sensitive to light polarization because they couple directly to the angular momentum carried by the radiation field [11].

In the presence of small amounts (~1%) of light absorbing dyes, such as MR, the director axis reorientation is greatly amplified due to changes in physical or chemical properties of dye molecules upon irradiation, consequently modifying the LC alignment through guest-host interaction [12]. Moreover, studies have shown that the liquid crystal refractive indices are practically impervious to the doping. The observed angular dependence can be broken out into two mechanisms. One mechanism is surface-mediated reorientation connected with the trans-cis isomerization of azo-dye molecules and the other mechanism is associated with photorefractive effects due to space charge modulation [13]. It was found that the structure of the dyes affects the reorientation efficiency as well as the orientation direction, where the host liquid crystals may reorient either parallel or perpendicular to the polarization of incident light [12].

Photoisomerization occurs when the azo-dye molecules are resonantly excited. Consequently, an additional torque is exerted on liquid crystals after anisotropic orientational distribution of trans and cis isomers are generated. In the presence of trans-cis photoisomerization there are three different molecular fields connected to the dye. The first two are the fields created by the ground-state trans and cis isomers; the third one is the molecular field of the excited-state molecules [10].

Photorefractive nonlinearities in liquid crystals arise from an incident optical intensity grating forming spatially modulated direct current (DC) space charge fields. The optical intensity grating is typically constructed by overlapping two coherent laser beams, which in turn form an interference pattern on the sample. Charge separation ensues in the bright regions of the interference pattern are followed by charge migration into the dark regions [14]. The two principal sources of space charge field formation include photo-induced conductivity inhomogeneity, which is similar to processes occurring in photorefractive crystals, and the Carr-Helfrich effect [15]. The DC space charges instigate torques on the nematic liquid crystal and thereby magnify the initial director axis reorientation. The

exceptionally nonlinear optical properties of dye-doped liquid crystals have emerged as promising image sensing and sensor protection materials.

In this document, we explore tuning of photonic structures including ring resonators and directional couplers with a reconfigurable liquid crystal cladding. A schematic of the devices appears in Figure 1. Ring resonators were demonstrated for various applications, including optical switching, selective filtering with small channel spacing, optical time delay, laser resonators, and photonic biosensors [16]. In electronic-photonic integrated chips, they form an integral part of back end photonic interconnect stack and they are suited for dense integration of optical networks.

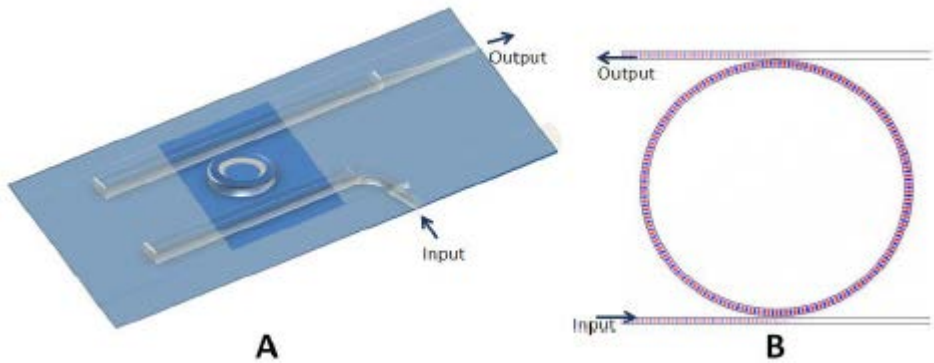

Figure 1. (A) Ring resonator. Windows for liquid crystal cladding are etched within the silicon dioxide over-cladding. (B) Simulation result showing critical coupling that translates to a resonance peak.

Our design, consisting of silicon strip waveguides surrounded by lower index liquid crystal cladding, confines the optical field energy to the high-index silicon regions. This approach capacitates high modal confinement and small ring size. However, the attuning effects of polymer may be enhanced when it is filled into the slot of a slot waveguide as compared to relying on the evanescent field to sense changes in the refractive index. Slot waveguides confine light in low-index-of-refraction regions and are typically based on a low-index submicrometer slot embedded between two silicon waveguides. Due to the high-index contrast, modes with strong field intensity at the two interfaces of the slot are formed. The overlap of the evanescent tail of the modes in the central slot leads to light confinement in the low-index region [17]. Nonetheless, most slot waveguides are significantly limited at high levels of waveguide loss ranging from 10- to 4-dB/cm, although Spott *et. al*. showed those limitations can be reduced to 2 dB/cm in the case of an asymmetric waveguide [18]. Other limitations of slot waveguides include the difficulty of integrating them with other chip-scale photonic elements, challenges in coupling to the input and output of a typical optical fiber, and the presence of quasi transverse electric (TE) and quasi transverse magnetic (TM) modes.

DESIGN AND ANALYTICAL MODEL

A number of liquid crystal properties are considered for this experiment. These include birefringence, positive or negative anisotropy, melting temperature, clearing temperature, and commercial availability. Typical birefringence ranges of commonly available nematics are on the order of $\Delta n = 0.05$ to $\Delta n = 0.25$, and these values are both temperature and wavelength dependent, with most having been characterized in the visible range. As the liquid crystal temperature rises towards the clearing temperature, the anisotropy decreases, even in the presence of an applied field (a good discussion of thermodynamics of liquid crystals in the presence of electromagnetic fields appears in [19]). Positive anisotropy liquid crystals are best suited for our application, due to the difficulties associated with homeotropic alignment of negative anisotropy LCs [20]. We chose 4-Cyano-4'-pentylbiphenyl (5CB) liquid crystal, which is a commonly used nematic, and when doped with MR dye, it exhibits a pronounced optical field reorientation. Since LCs themselves are not highly sensitive to light, they require doping with Azo dyes, such as MR, for the photophysical and photochemical transformations to take place. Under ultraviolet (UV) illumination, the Azo dye undergoes a reorientation in the direction normal to the incident light polarization while simultaneously exerting a torque on the liquid crystal molecules causing them to align in the direction of dye alignment [21]. 5CB anisotropy is $\Delta n = 0.24$ at room temperature and at 1550 nm, the LC undergoes a phase transition from a crystalline state to a nematic state at 22.5 °C and it transitions from a nematic to an isotropic state at 35 °C. Photoalignment liquid crystals are easy to work with and minimize fabrication time because they are non-contact and do not require an alignment layer. Generally, the alignment layer is created by a mechanical rubbing process of the film that the liquid crystals come into contact with. This commonly used method results in grooves being formed along the rubbing direction where liquid crystals align themselves down the groove path. However, the rubbing process frequently generates grooves much larger than liquid crystal molecules ensuing in an inefficient alignment, in addition to introducing scratches, electrostatic charges, and other damage to the surface.

To study the attributes of 5CB cladded structures, two-dimensional finite-element simulations were implemented in COMSOL® Multiphysics software for both the TE and TM configurations. COMSOL Multiphysics is based on finite element analysis. It is well suited for modeling the propagation of electromagnetic waves in photonic waveguides. The effective index method was used to help define the effective mode indices and propagation constants for the TE and TM modes of our ring resonator.

A ring resonator is typically formed by looping an optical waveguide back on itself such that it forms a ring. Coupling to the device is achieved by placing a bus waveguide adjacent to the ring at a distance allowing for an evanescent mode overlap. A resonance occurs when the optical path length of the resonator is exactly a whole number of wavelengths and the spacing between the resonances is referred to as the free spectral range (FSR) [22]. In the presence of varying refractive indices, a shift of the resonance wavelength takes place due to a change of the effective index of the resonant mode n_{eff} [23]. It can be described by

$$\Delta\lambda = \frac{L}{m}\Delta n_{eff(\lambda_1-\lambda_2)} \tag{6}$$

where m indicates the order of the resonance, L is the circumference of the resonator, and λ is the free-space wavelength of the resonance frequency.

The ring resonator devices consisted of two 550-nm wide, 30-µm long waveguides separated by 100 nm from a 19.8-µm-diameter ring (also 550-nm wide). The ring was situated directly between the waveguides; a schematic of the devices is portrayed in Figure 1. Tuning of the ring resonator depends on how far the mode extends into the cladding regions, the amount of space in the coupling region between the ring and waveguide, the accrued losses (including coupling to bus waveguides), as well as the initial alignment of liquid crystals. The silicon dioxide cladding covered a third of the ring to break the ring symmetry. Theoretical analysis showed that at room temperature, the ring resonator sustains a resonance shift of 46.1 and 17.1 nm for TM and TE modes, respectively. The evanescent field of TM modes extends farther into the cladding regions as compared to the TE evanescent field, thereby TM modes in the strip waveguides are more susceptible to the LC birefringence effects. The simulated result appears in Figure 2.

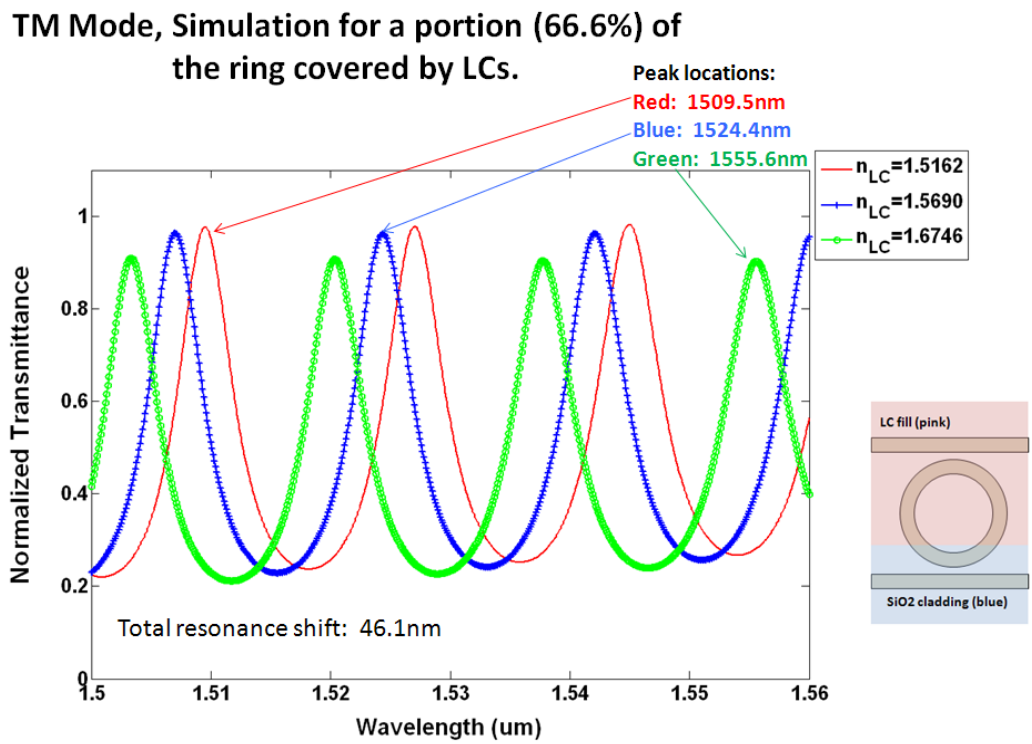

Figure 2. (A,B) Simulation result for the TE mode, (B) the simulated ring resonator structure and its TM mode response.

To validate the feasibility of optical tuning, a preliminary measurement aimed at showing that it is possible to affect the device response by changing the index of the cladding was performed.

DEVICE FABRICATION AND CHARACTERIZATION

Samples were fabricated using a silicon-on-insulator (SOI) wafer composed of a 250-nm silicon layer positioned on top of 3-µm SiO_2 and with a silicon handle, for a total wafer thickness of 680 µm. The 3-µm buried oxide layer aids in preventing the evanescent field of the optical mode from penetrating the silicon substrate below. A 120-nm thick coat of hydrogen silsesquioxane (HSQ) resist spun on the wafer and patterned with electron beam lithography (EBL) served as a mask for the dry etch of silicon. The specific resist used was Dow Corning FOX-16, and it was diluted in methyl isobutyl ketone (MIBK) as 1 part FOX-16 to 3 parts MIBK (by weight) and spun at 5000 rpm. The samples were then exposed via a JEOL JBX-5D11 system and dry etched using Oxford Plasmalab® 100 Inductively Coupled Plasma Reactive Ion Etching (ICP RIE).

The resulting silicon waveguides were covered by a 1.8-um layer of SiO_2 cladding deposited via plasma-enhanced chemical vapor deposition (PECVD). Window areas for liquid crystals were patterned with S1805 photoresist, exposed in a HTG Mask Aligner and etched in a buffered oxide solution (1:6 buffered oxide etch). The remaining S1805 photoresist was removed with acetone. The fabrication process of photo alignment samples is depicted in Figure 3, and the fabricated structures are shown in Figure 4.

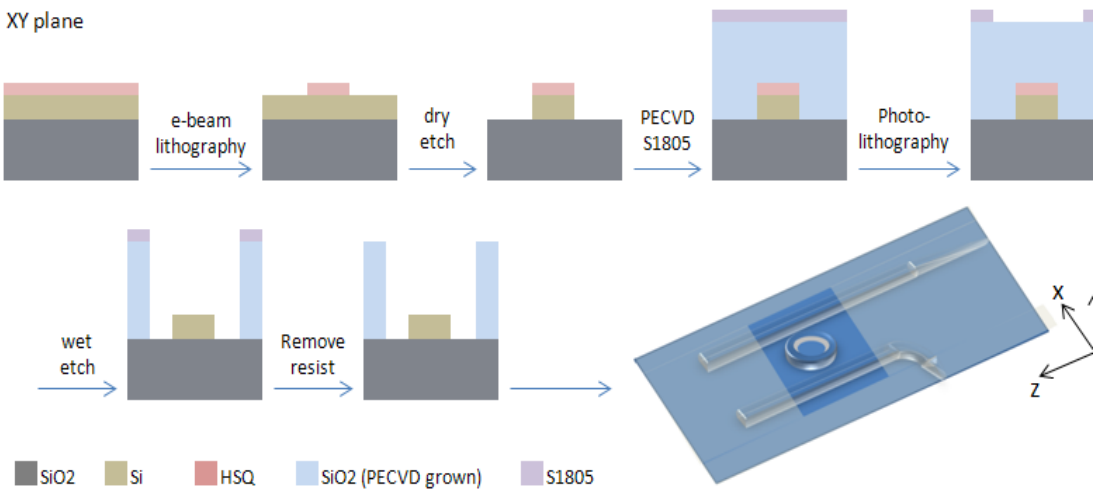

Figure 3. Fabrication process steps for devices with a photo-voltage liquid crystal cladding. The dimensions are not to scale.

Linear inverse tapers were implemented for both the photo-alignment and voltage alignment samples to aid in the coupling from an optical fiber to the on-chip waveguide. The adiabatically widened tapers, where the 100-nm tip of the taper slowly increases into the 550-nm wide waveguide over the course of 100 µm, work by increasing the mode size of the waveguide to that of the fiber. These structures offer a robust and low-loss coupling mechanism. For a 100-nm tip, 100-µm long linear inverse taper, the predicted loss is on the order of 1.5 dB [24].

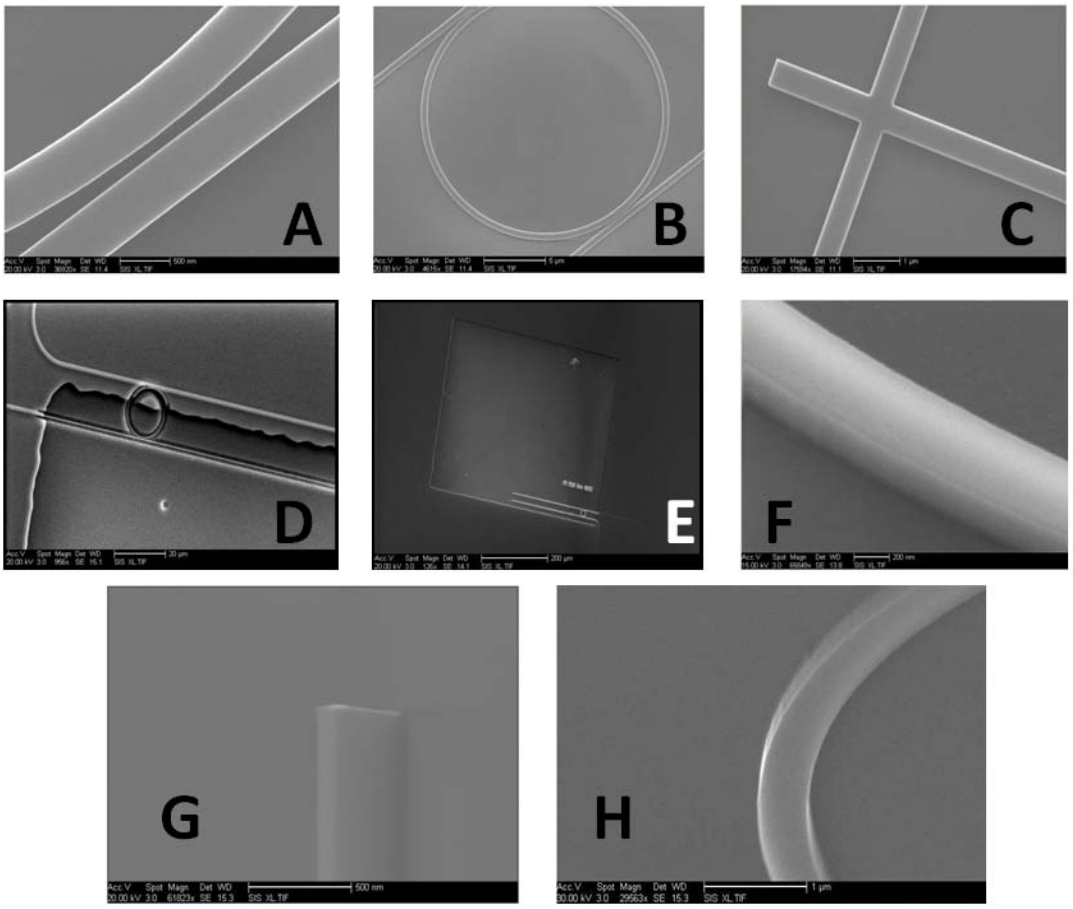

Figure 4. Fabricated ring resonator structures. (A) Gap between the ring and bus waveguide; (B) Ring resonator; (C) Fabricated leads for electrodes; (D, E) Etched silicon dioxide cladding to allow room for liquid crystals; (F) 45-degree view of the waveguide sidewalls (250-nm tall); (G) Tip of the inverse taper; (H) 85-degree view of the ring sidewalls.

The experimental setup consisted of a thermoelectric module coupled to Oven Industries 5C7-195 Benchtop Temperature Controller for heating and cooling of the liquid crystal mixture. The thermoelectric module was placed on a three-axis mechanical stage, allowing for precise alignment of the sample with the input beam and imaging optics. The transmission spectrum was measured with a tunable Agilent 8163B telecom-grade laser (1470- to 1570-nm range) connected to a polarization scrambler and fiber coupled to the on-chip waveguide. Waveguide output was free-space imaged onto a power meter. While the free-space output of the measurement setup is prone to jitter, it is easy to construct, reconfigure, and align. A polarizer in the output path allowed for a selection of TE transmission (horizontal polarization) or TM transmission (vertical polarization). Control of the telecommunications source, the power meter, and the source step size was automated. The typical step size was 20 pm.

Linear inverse tapers were implemented for both the photo alignment and voltage alignment samples to aid in the coupling from an optical fiber to the on-chip waveguide. The adiabatically widened tapers, where the 100-nm tip of the taper slowly increases into the 550-nm wide waveguide over the course of 100 µm, work by increasing the mode size of the

waveguide to that of the fiber. These structures offer a robust and low-loss coupling mechanism. For a 100-nm tip, 100-µm long linear inverse taper, the predicted loss is on the order of 1.5 dB [23].

A 470-nm Mightex light emitting diode (LED) source coupled with a polarizer and a quarter-wave plate was focused onto the sample with a plano-convex lens. The quarter-wave plate, in conjunction with the polarizer, allowed for linear or circular polarization of the LED source. The output power irradiating the sample was 85 µW with a spot size of 0.49 cm^2. Note that the liquid crystal realignment depends on the UV source dosage, and not on the intensity alone. The experimental setup is shown in Figure 5.

Nematic 5CB liquid crystals mixed with MR dye at a 1% concentration of MR were used in the experiment. A drop of liquid crystal material was placed onto the window regions of the sample and heated at 40 °C (above isotropic temperature of 5CB) for 10 minutes in order for the liquid crystal material to completely fill the cell, then cooled back to room temperature. The 470-nm source was enabled, and the quarter-wave plate and linear polarizer were set to result in circular polarization to randomize the liquid crystal orientation. The polarization of the tunable Agilent source was set to TE. A measurement was executed, followed by a reorientation of the 470-nm source polarization corresponding to liquid crystal alignment in the direction parallel to the silicon waveguides. A second measurement set was performed. The polarization was then set to allow for liquid crystal orientation to be perpendicular to the silicon waveguides, and a third measurement was taken.

Our preliminary measurement results, appearing in Figure 6, yield a 5.6-nm resonance shift due to the liquid crystal cladding change between n_o and n_e, where the location of the resonance was calculated using center of mass, which provides for higher accuracy as compared to tracking the peak value. The resonance shift is considerably smaller as compared to the modeled result of 17.1 nm, stemming from the modeling software's inability to account for individual liquid crystal molecule orientations or the anchoring energy of liquid crystals at the silicon interface. The software model only considers the best-case scenario where the liquid crystal refractive index has an absolute correspondence to n_o or n_e values.

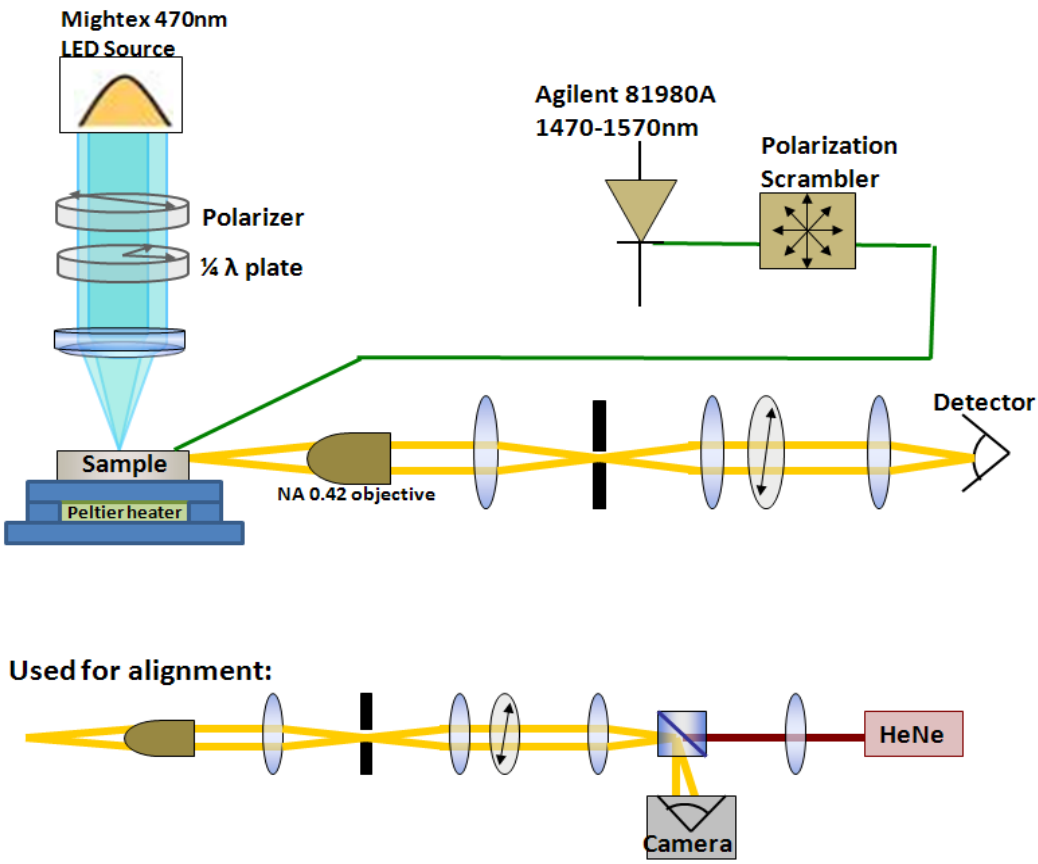

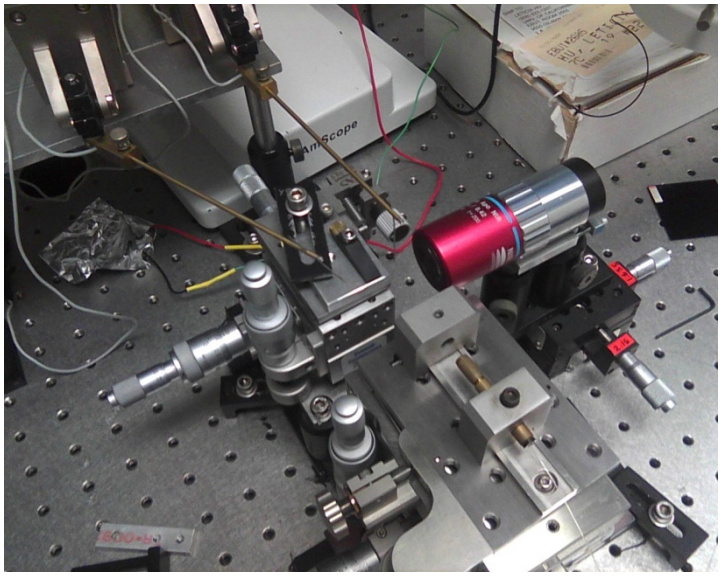

Figure 5. Experimental setup.

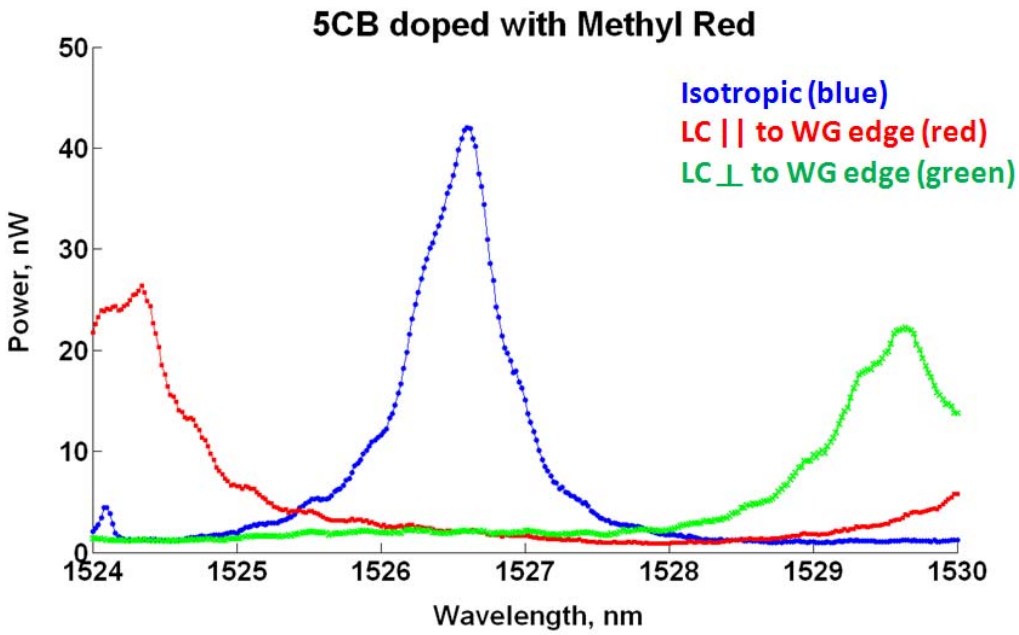

Figure 6. Experimental results of 5CB liquid crystal doped with methyl red dye.

SUMMARY

In conclusion, the feasibility of photo-tuning of silicon photonic structures clad in nematic liquid crystals under low-intensity UV irradiation was presented theoretically and verified experimentally. Tunable optical circuit components are one of the essential technologies in the development of photonic analogues for classical electronic devices, and as silicon photonics and all-optical platforms advance, optically tunable devices are poised to play an increasingly central role.

REFERENCES

1. I. C. Khoo, M. V. Wood, M. Y. Shih, and P. H. Chen. 1999. "Extremely Nonlinear Photosensitive Liquid Crystals for Image Sensing and Sensor Protection," *Optics Express* **4:**432–442.

2. J. Cos, J. Ferré-Borrull, J. Pallarès, and L. F. Marsal. 2011. "Tunable Waveguides Based on Liquid Crystal-Infiltrated Silicon Photonic Crystals," *Phys. Status Solidi C* **8:**1075–1078.

3. A. W. Domanski, D. Budaszewski, M. Sierakowski, and T. R. Wolinski. 2006. "Depolarization of Partially Coherent Light in Liquid Crystals," *Opto-Electronics Review* **14:**305–310.

4. V. R. Almeida, C. A. Barrios, R. R. Panepucci, and M. Lipson. 2004. "All-optical Control of Light on a Silicon Chip," *Nature* **431:**1081–1084.

5. S. M. Weiss and P. M. Fauchet. 2005. "Active Building Blocks for Silicon Photonic Devices," *Proc. SPIE:*6017, 60170H.

6. P. Yeh and C. Gu. 1999. *Optics of Liquid Crystal Displays.* John Wiley and Sons, Inc., Hoboken, NJ.

7. L. M. Blinov. 2011. *Structure and Properties of Liquid Crystals.* Springer Science Business Media.

8. P. Oswald and P. Pieranski. 2005. *Nematic and Cholesteric Liquid Crystals: Concepts and Physical Properties Illustrated by Experiments.* CRC Press, Taylor & Francis Group, Boca Raton, FL.

9. I. Janossy. 1994. "Molecular Interpretation of the Absorption-Induced Optical Reorientation of Nematic Liquid Crystals," *Physical Review E* **49:**2957–2963.

10. I. Janossy and L. Szabados. 1998. "Optical Reorientation of Nematic Liquid Crystals in the Presence of Photoisomerization," *Physical Review E* **58:**4598–4604.

11. L. Marrucci, P. Maddalena, G. Arnone, L. Sirleto, and E. Santamato. 1997. "Liquid Crystal Reorientation Induced by Completely Unpolarized Light," *Physical Review E* **57:**3033–3037.

12. H. Zhang, S. Shiino, O. Tsutsumi, A. Kanazawa, T. Shiono, and T. Ikeda. 2001. "Photoinduced Reorientation of Liquid Crystals Doped with a Mesogenic Oligothiophene," *Mol. Cryst. and Liq. Cryst.* **368:**369–376.

13. A. Petrossian and S. Residori. 2002. "Surfactant Enhanced Reorientation in Dye-doped Nematic Liquid Crystals," *Europhys. Lett.* **60:**79–85.

14. G. P. Wiederrecht. 2001. "Photorefractive Liquid Crystals," *Annu. Rev. Mater. Res.* **31:**139–169.

15. I. C. Khoo. 1996. "Orientational Photorefractive Effects in Nematic Liquid Crystal Films," *IEEE Jour. Quantum Electronics* **32:**525–534.

16. J. E. Heebner, V. Wong, A. Schweinsberg, R. W. Boyd, and D. J. Jackson. 2004. "Optical Transmission Characteristics of Fiber Ring Resonators," *IEEE Journal of Quantum Electronics* **40:** 726–730.

17. M. Lipson. 2005. "Guiding, Modulating, and Emitting Light On Silicon—Challenges and Opportunities," *Journal of Lightwave Technology* **23:**4222–4238.

18. A. Spott, T. B. Jones, R. Ding, Y. Liu, R. Bojko, T. O'Malley, A. Pomerene, C. Hill, W. Reinhardt, and M. Hochberg. 2011. "Photolithographically Fabricated Low-Loss Asymmetric Silicon Slot Waveguides," *Optics Express* **19:**10950.

19. A. Morro. 2009. "Modeling of Nematic Liquid Crystals in Electromagnetic Fields," *Advances in Theoretical and Applied Mechanics* **2:**43–58.

20. L. Z. Ruan, F. Yang, and J. R. Sambles. 2008. "Voltage Dependent Director of a Homeotropic Negative Liquid Crystal Cell," *Applied Physics Letters* **93:**031909.

21. B. Zhang, K. K. Li, V. Chigrinov, H. S. Kwok, and H. C. Huang. 2005. "Application of Photoalignment Technology to Liquid-Crystal-on-Silicon Microdisplays," *Jpn. J. Appl. Phys.* **44:** 3983–3991.

22. W. Bogaerts, P. De Heyn, T. Van Vaerenbergh, K. DeVos, S. K. Selvaraja, T. Claes, P. Dumon, P. Bienstman, D. Van Thourhout, and R. Baets. 2012. "Silicon Microring Resonators," *Laser Photonics Rev.* **6:** 47–73.

23. T. Baehr-Jones, M. Hochberg, C. Walker, E. Chan, D. Koshinz, W. Krug, and A. Scherer. 2005. "Analysis of the Tuning Sensitivity of Silicon-on-Insulator Optical Ring Resonators," *Journal of Lightwave Technology* **23:**4215-4221.

24. G. Ren, S. Chen, Y. Cheng, and Y. Zhai. 2001. "Study on Inverse Taper Based Mode Transformer for Low Loss Coupling between Silicon Wire Waveguide and Lensed Fiber," *Optics Communications* **284:**4782–4788.

REPORT DOCUMENTATION PAGE

Form Approved
OMB No. 0704-01-0188

The public reporting burden for this collection of information is estimated to average 1 hour per response, including the time for reviewing instructions, searching existing data sources, gathering and maintaining the data needed, and completing and reviewing the collection of information. Send comments regarding this burden estimate or any other aspect of this collection of information, including suggestions for reducing the burden to Department of Defense, Washington Headquarters Services Directorate for Information Operations and Reports (0704-0188), 1215 Jefferson Davis Highway, Suite 1204, Arlington VA 22202-4302. Respondents should be aware that notwithstanding any other provision of law, no person shall be subject to any penalty for failing to comply with a collection of information if it does not display a currently valid OMB control number.
PLEASE DO NOT RETURN YOUR FORM TO THE ABOVE ADDRESS.

1. REPORT DATE *(DD-MM-YYYY)*
March 2013

2. REPORT TYPE
Final

3. DATES COVERED *(From - To)*

4. TITLE AND SUBTITLE

Absorption-induced Optical Tuning of Silicon Photonic Structures Clad with Nematic Liquid Crystals

5a. CONTRACT NUMBER

5b. GRANT NUMBER

5c. PROGRAM ELEMENT NUMBER

5d. PROJECT NUMBER

5e. TASK NUMBER

5f. WORK UNIT NUMBER

6. AUTHORS

J. N. Ptasinski

7. PERFORMING ORGANIZATION NAME(S) AND ADDRESS(ES)

SSC Pacific
5622 Hull Street
San Diego, CA 92152–5001

8. PERFORMING ORGANIZATION REPORT NUMBER

TD 3268

9. SPONSORING/MONITORING AGENCY NAME(S) AND ADDRESS(ES)

Office of Naval Research
800 North Quincy Street
Arlingtom, VA 2217-5000

10. SPONSOR/MONITOR'S ACRONYM(S)

11. SPONSOR/MONITOR'S REPORT NUMBER(S)

12. DISTRIBUTION/AVAILABILITY STATEMENT

Approved for public release.

13. SUPPLEMENTARY NOTES

This is work of the United States Government and therefore is not copyrighted. This work may be copied and disseminated without restriction.

14. ABSTRACT

Theoretical and experimental analysis of active, absorption induced optical tuning of silicon photonic devices using silicon strip waveguides combined with nematic liquid crystal (NLC) claddings. Tuning of the silicon structures is performed under low power photo irradiation, which offers a very simple way to control the spectral response of ring resonator devices.

15. SUBJECT TERMS

silicon photonics
nematic liquid crystals
optical tuning
ring resonator
tunable optical circuit
photo-tuning

16. SECURITY CLASSIFICATION OF:			17. LIMITATION OF ABSTRACT	18. NUMBER OF PAGES	19a. NAME OF RESPONSIBLE PERSON
a. REPORT	b. ABSTRACT	c. THIS PAGE			J. N. Ptasinski
U	U	U	U	26	19B. TELEPHONE NUMBER *(Include area code)* (619) 553-3727

Standard Form 298 (Rev. 8/98)
Prescribed by ANSI Std. Z39.18

INITIAL DISTRIBUTION

84300	Library	(2)
85300	Archive/Stock	(1)
85300	J. N. Ptasinski	(10)

Defense Technical Information Center
Fort Belvoir, VA 22060–6218 (1)

Approved for public release.

SSC Pacific
San Diego, CA 92152-5001